Longitudinal absorption and interferometric measurements at Wigner RCP

SCHEME

- Ti-Sapphire laser beam propagating longitudinally through the Rb-cell
- Counterpropagating quasi-resonant diode laser beam
- Detection of absorption (transmission) and interferometric signals:
  - Vs time: fast photodetector
  - Lateral distribution: gated camera

1. Temporal dependence of absorption and interferometric signals measured with the Legend laser (3 mJ, 40 fs)

(G.P. Djotyan et al., Nucl. Instr. Meth. A 884 (2018) 25-30)

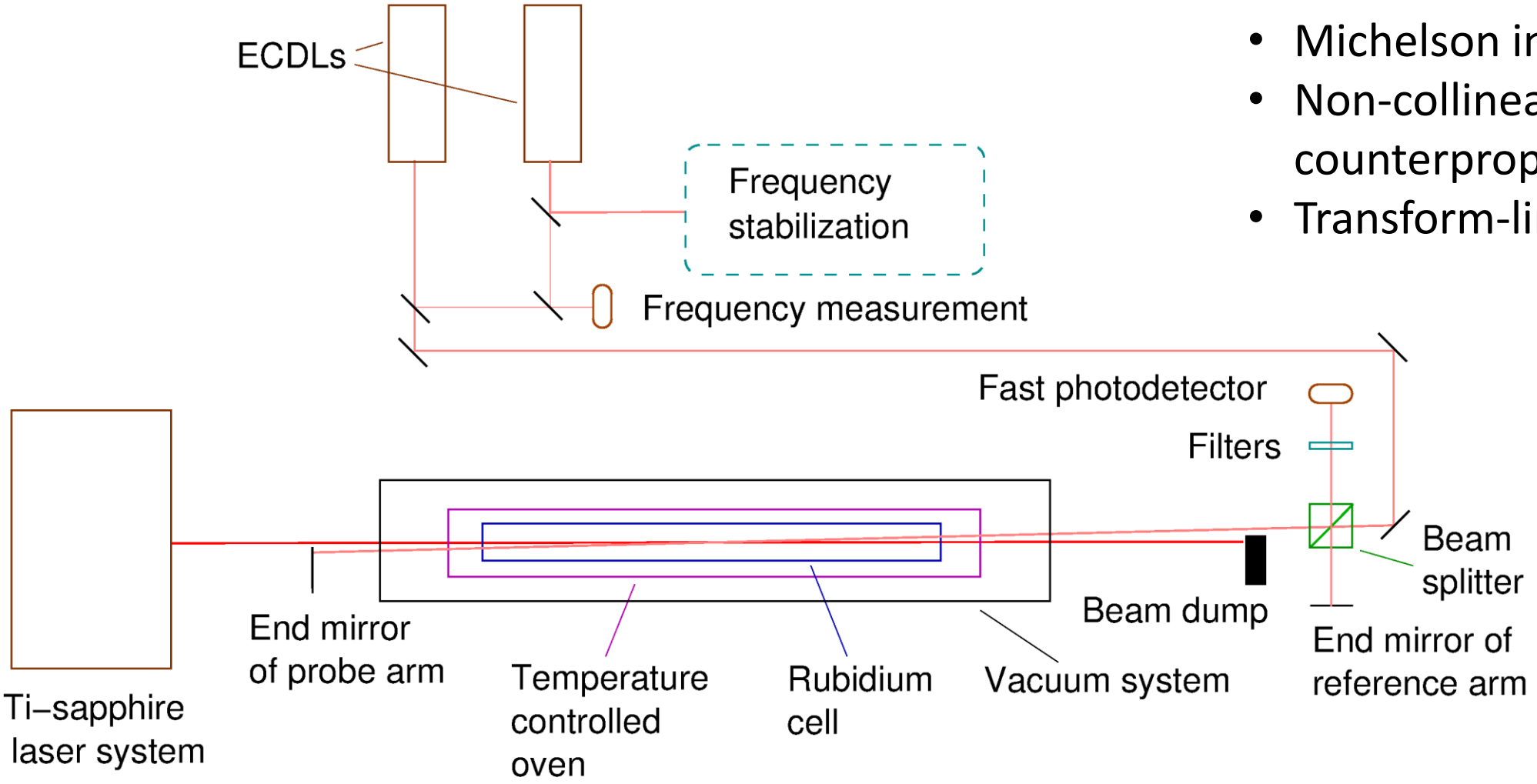

- Michelson interferometer
- Non-collinear counterpropagating beams
- Transform-limited pulses

Interferometric signals with fitted exponentially decaying phase difference

$$I_{\mathrm{interf}}(t) = I_{\mathrm{tr}}(t) + I_{\mathrm{ref}} + 2\epsilon\sqrt{I_{\mathrm{tr}}(t)I_{\mathrm{ref}}} \cdot \cos(\varphi_0 + \varphi_1(t)) \qquad \varphi_1(t) = \varphi_1^{(0)} \mathrm{e}^{-t/\tau}$$

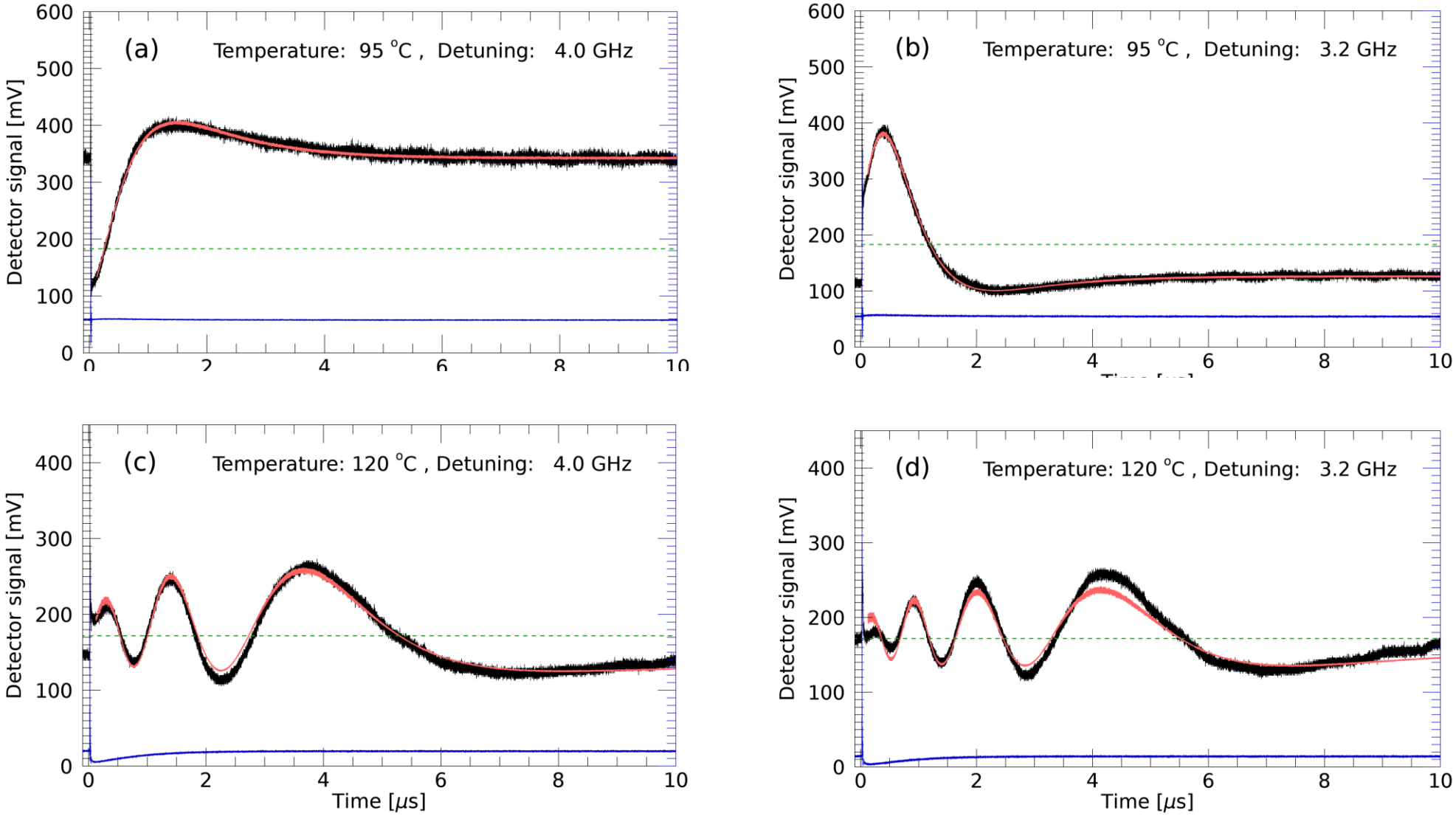

Results of the density calculations

$$\Delta N_{\mathrm{p}}(t)L = \varphi_1(t)\frac{\lambda_{\mathrm{L}} m}{\pi^2 f e^2}\left[\sum_{i=1}^{2} p_i \sum_{j=1}^{2} \frac{\Delta\omega_j^{(i)}}{\omega_{0j}^{(i)}(\Delta\omega_j^{(i)2} + \Gamma^2)}\right]^{-1}$$

Temperature (°C)	95		120	
Detuning (GHz)	4.0	3.2	4.0	3.2
$\varphi_1^{(0)}$ (rad)	3.59	5.41	18.3	24.8
τ (μs)	1.08	1.07	2.28	2.31
ΔN_{p} (cm^{-3})	3.5×10^{11}	4.6×10^{11}	1.8×10^{12}	2.1×10^{12}
$\Delta N_{\mathrm{p}}/N$ (%)	8.1	10.6	8.8	10.4

2. Experiments with the Hidra laser (30 mJ, 40 fs)

- Mach-Zehnder interferometer
- Collinear counterpropagating beams
- Chirped pulses (~300 fs)

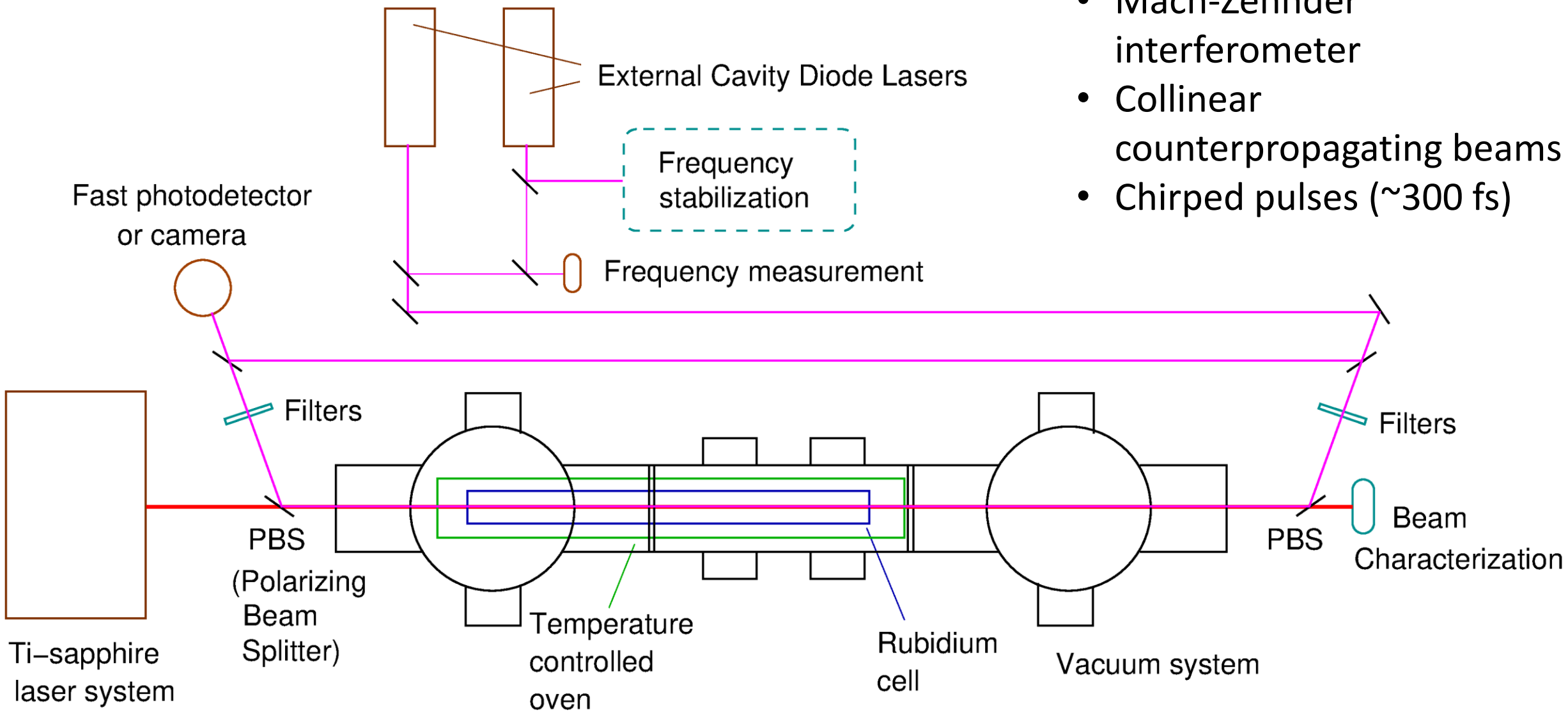

Temporal dependence of the transmission and interference signals

Difference between the efficiency of the pulses with positive and negative chirp: NEGATIVE CHIRP is more efficient

Ti:Sa laser pulse energy: 13.5 mJ; Diode laser detuning: -1 GHz

Positive chirp

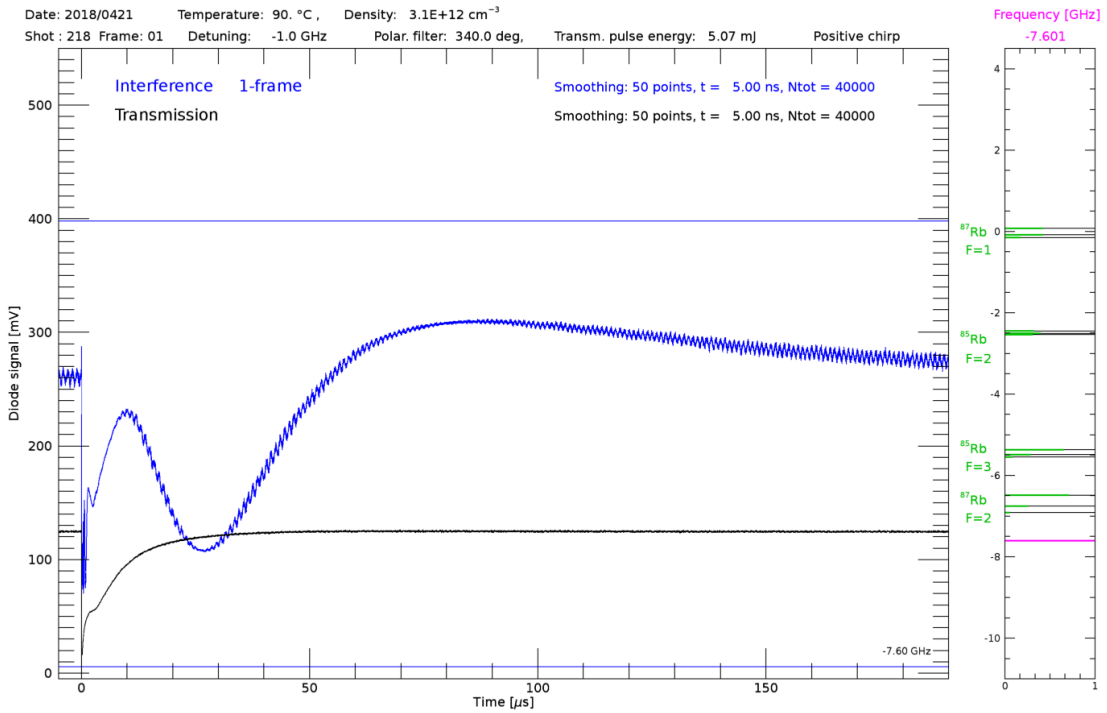

Negative chirp

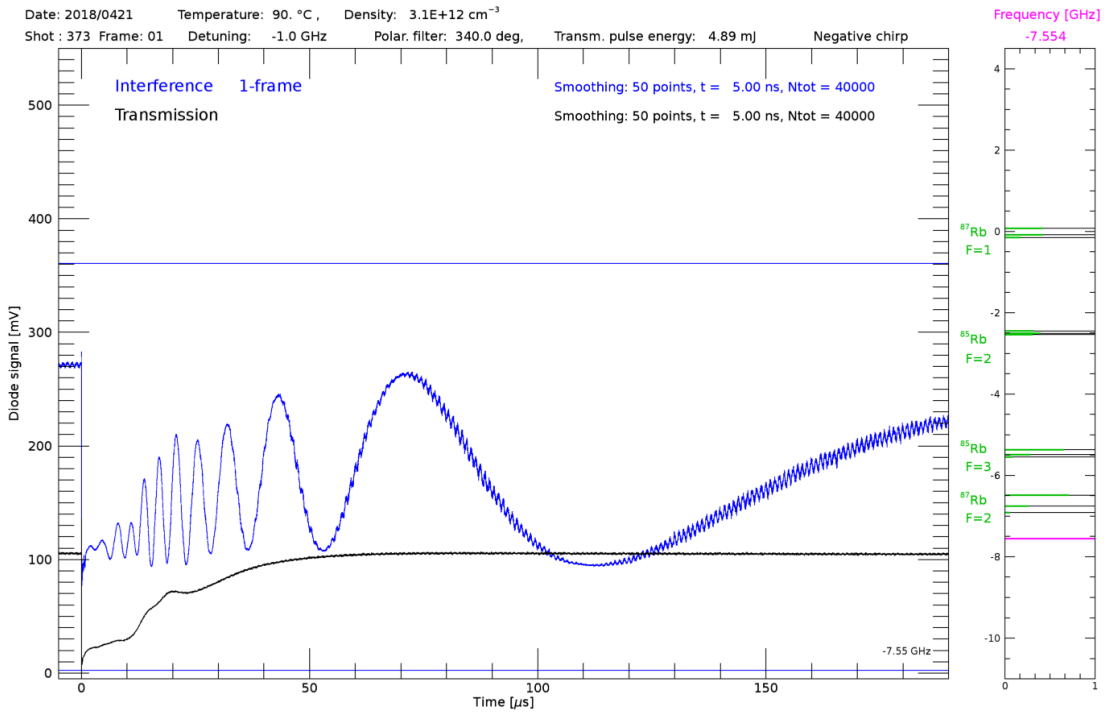

Transmission signals are different for positive and negative diode laser detuning

→ focusing / defocusing of the transmitted beam ?

Ti:Sa laser: pulse energy: 13.5 mJ, negative chirp

Diode laser:

Negative detuning: -1 GHz

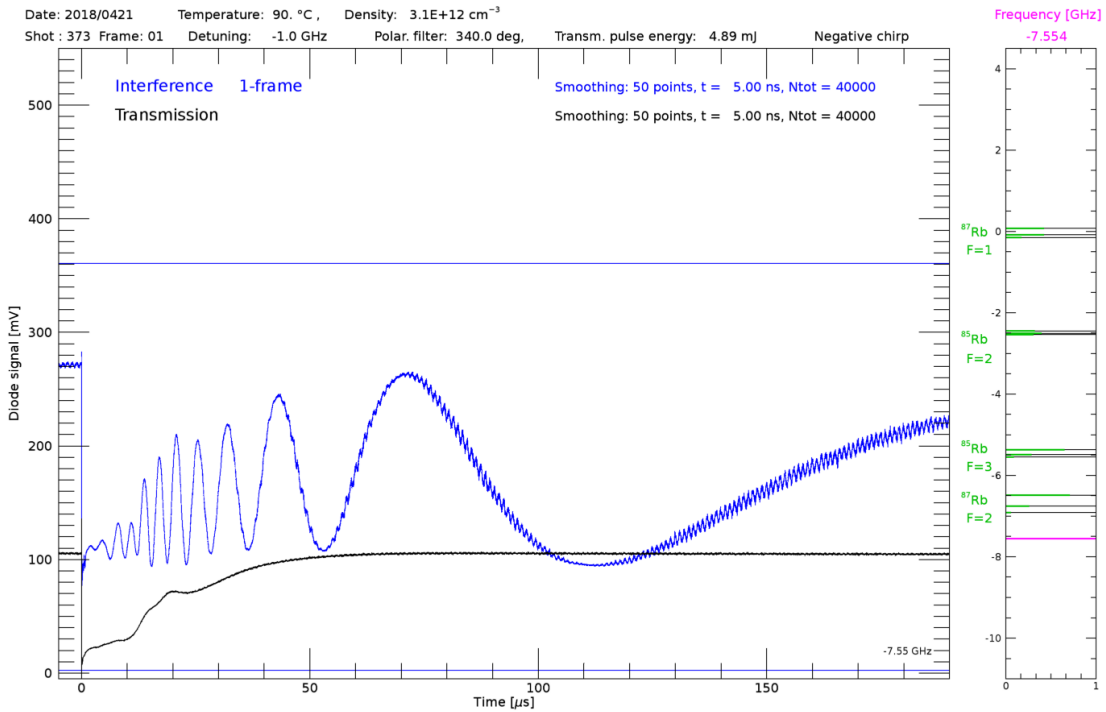

Positive detuning: +1 GHz

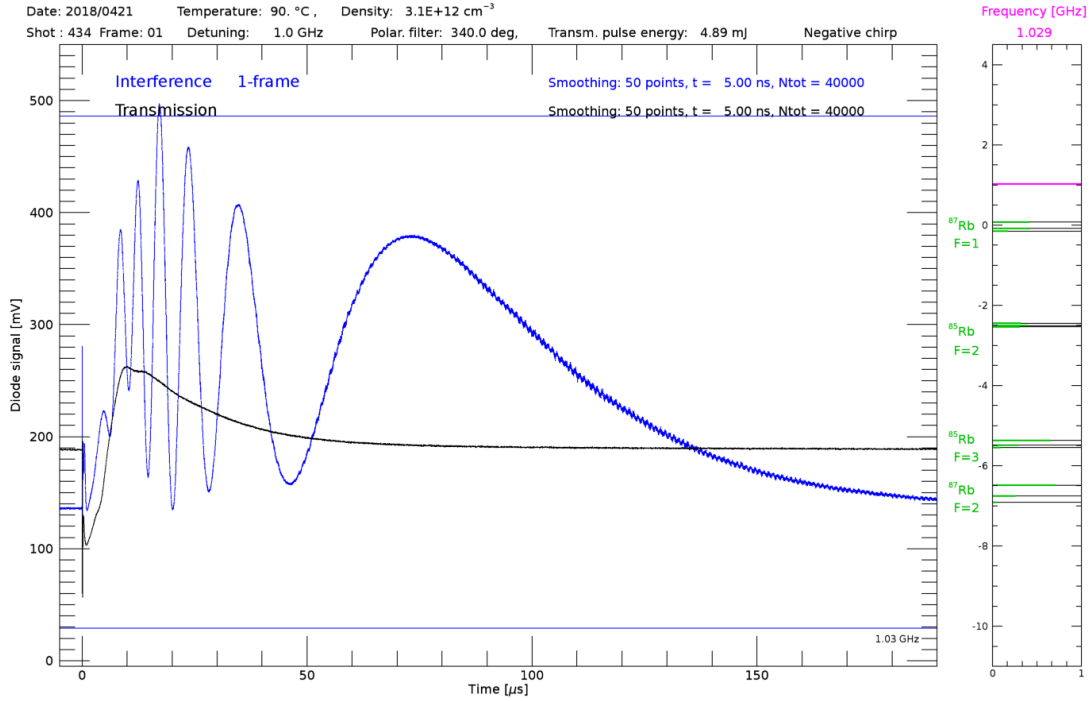

Measurement of the lateral distribution of the transmitted diode laser beam intensity and interferograms with a gated camera at different delay times after the Ti:Sa pulse

(Exposure time of the image intensifier: 200 ns)

Positive detuning → lower refractive index of the vapor
density is lower at the middle → positive lens → focusing

Negative detuning → higher refractive index of the vapor
density is lower at the middle → negative lens → defocusing

Interference signals → ring structure varying in time → calculation of the density distribution

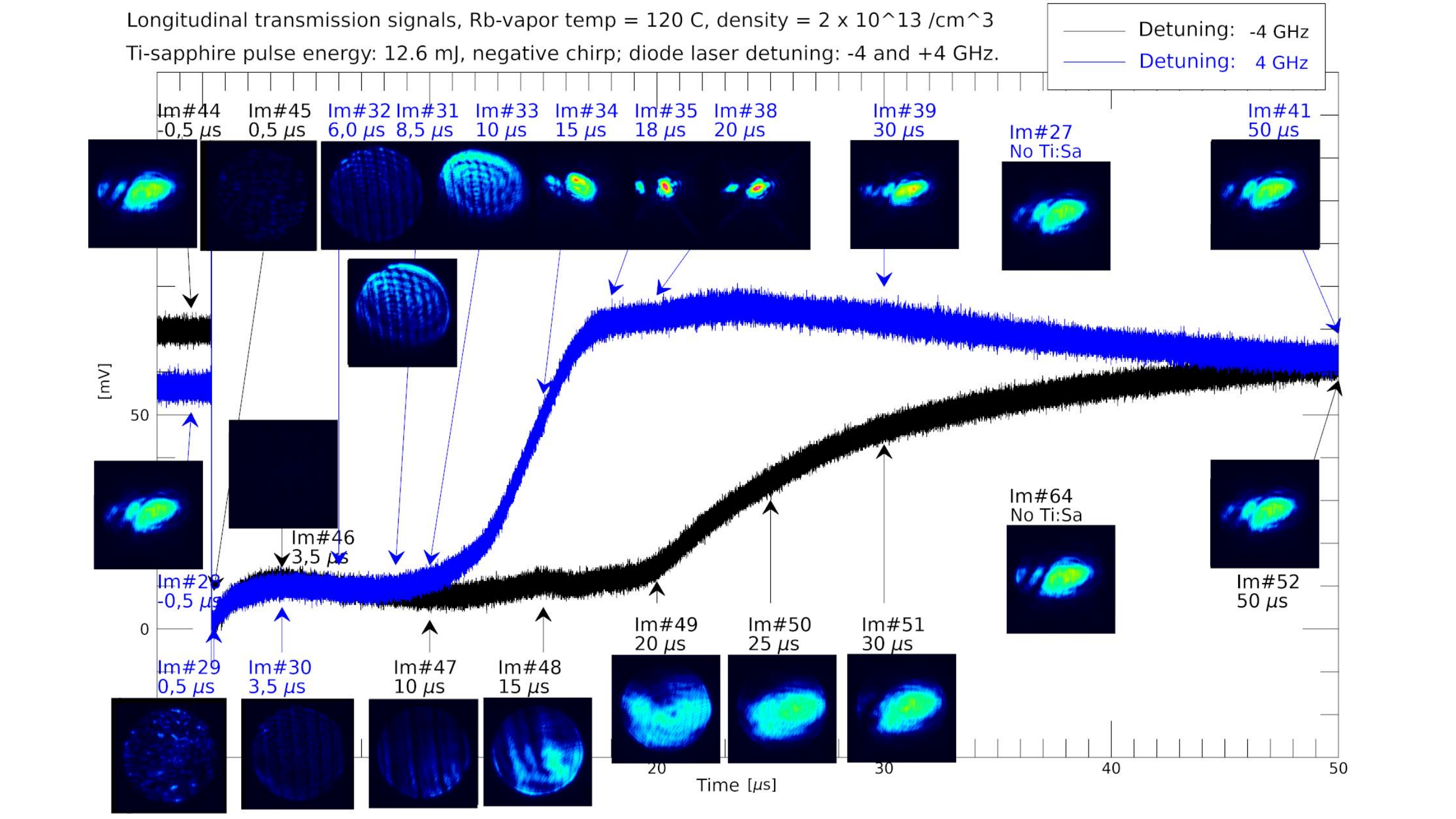
Longitudinal transmission signals, Rb-vapor temp = 120 C, density = 2 x 10^13 /cm^3
Ti-sapphire pulse energy: 12.6 mJ, negative chirp; diode laser detuning: -4 and +4 GHz.
Detuning: -4 GHz
Detuning: 4 GHz
Im#44 -0,5 μs
Im#45 0,5 μs
Im#32 6,0 μs
Im#31 8,5 μs
Im#33 10 μs
Im#34 15 μs
Im#35 18 μs
Im#38 20 μs
Im#39 30 μs
Im#27 No Ti:Sa
Im#41 50 μs
[mV]
50
0
Im#46 3,5 μs
Im#28 -0,5 μs
Im#64 No Ti:Sa
Im#52 50 μs
Im#29 0,5 μs
Im#30 3,5 μs
Im#47 10 μs
Im#48 15 μs
Im#49 20 μs
Im#50 25 μs
Im#51 30 μs
20
30
40
50
Time [μs]

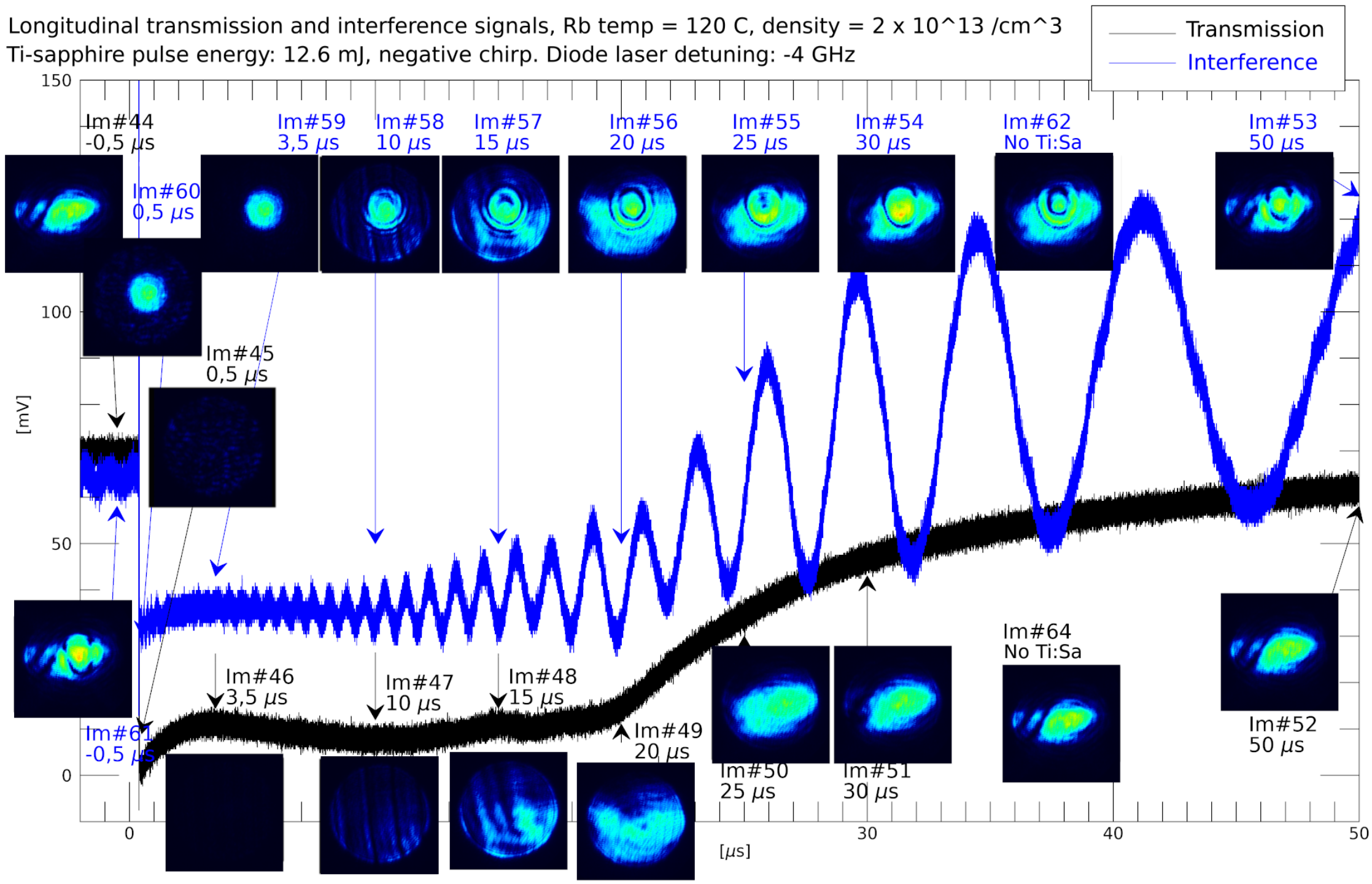
Longitudinal transmission and interference signals, Rb temp = 120 C, density = 2 x 10^13 /cm^3
Ti-sapphire pulse energy: 12.6 mJ, negative chirp. Diode laser detuning: -4 GHz
Transmission
Interference
Im#44
-0,5 μs
Im#60
0,5 μs
Im#59
3,5 μs
Im#58
10 μs
Im#57
15 μs
Im#56
20 μs
Im#55
25 μs
Im#54
30 μs
Im#62
No Ti:Sa
Im#53
50 μs
Im#45
0,5 μs
Im#61
-0,5 μs
Im#46
3,5 μs
Im#47
10 μs
Im#48
15 μs
Im#49
20 μs
Im#50
25 μs
Im#51
30 μs
Im#64
No Ti:Sa
Im#52
50 μs
[mV]
[μs]
150
100
50
0
0
30
40
50